

# Optimal Control of Battery Fast Charging Based-on Pontryagin's Minimum Principle

Saehong Park, Donggun Lee, Hyoung Jun Ahn, Claire Tomlin, Scott Moura

**Abstract**—This paper derives provably optimal control trajectories for the Li-ion battery fast charging problem. Conventionally, battery charging protocols must satisfy safety constraints while maximizing the state of charge (SoC) level. In the literature, both computational and experimental studies promote a diversity of algorithms, including pulse charging, multi-step constant currents, and more. Although these approaches yield applicable charging algorithms, the literature lacks a rigorous analytical insight into optimal charging trajectories. In this paper, we focus on the Pontryagin's Minimum Principle for solving optimal control problem for battery fast charging. Specifically, we characterize the optimal control solution with respect to the state constraint bound. The optimal input is analytically derived for a reduced-order electrochemical model. The optimal solutions follow a *Bang* or *Bang-Ride* trajectory. Numerical simulations validate the analytical solutions.

**Keywords**—Constrained Optimal Control, Pontryagin Minimum Principle, Electrochemical model, Battery fast charging,

## I. INTRODUCTION

Battery fast charging performs an essential role in electrified transportation to reduce driver's waiting time and range anxiety. This can be easily achieved by using aggressive current profiles, however, it also accelerates battery degradation effects, such as solid electrolyte interface layer growth, and lithium plating deposition. For this reason, batteries should be carefully monitored and controlled during fast charging as it may cause cells to crack, leak, and lose capacity. The role of battery management systems is to charge the batteries as fast as possible while not violating the safety constraints. In the literature, several model-based optimal control techniques have been proposed in consideration of providing fast-charging while guaranteeing safety constraints.

The authors in [1] formulate a minimum-time charging problem and use nonlinear model predictive control. Similarly, authors in [2] propose quadratic dynamic matrix control formulation to design an optimal charging strategy for real-time model predictive control. In the context of aging mechanism, the authors of [3] have studied the trade-off between charging speed and degradation, based on an electro-thermal-aging model. The authors in [4] consider minimizing film layer growth of the electrochemical model. Authors in [5] derive an optimal current profile using a single particle

model with intercalation-induced stress generation. The key novelty here is incorporating mechanical fracture, which can be a dominant mechanism in degradation and capacity fade. To ensure safety, a proportional–integral–derivative controller is proposed. In [6], the authors exploit differential flatness properties of the single particle model to yield a computationally efficient optimal control problem, solved via pseudospectral methods. On the other hand, the authors in [7] synthesize a state estimation and model predictive control scheme for a reduced electrochemical-thermal model, in order to design health-aware fast charging strategy. The problem is formulated as a linear time-varying model predictive control scheme, with a moving horizon state estimation framework. Similarly, authors of [8] propose reference governor approach for equivalent hydraulic battery model, which integrates state estimation with a reference governor scheme.

Nearly all existing model-based control strategies apply computational methods that yield the following: apply maximal charging current until the battery reaches one of the constraints, and then ride this constraint. There are a number of research papers showing this rule empirically. However, a theoretical analysis that derives and characterizes this solution has not been executed.

To solve a deterministic optimal control problem, there are two related methods: (i) the Hamilton-Jacobi-Bellman (HJB), which is based on Bellman's principle of optimality [9], and (ii) Pontryagin Minimum Principle (PMP), which originates from *Calculus of Variations*. The HJB approach guarantees the global optimal solution. Often, the solution to the HJB PDE is computed by the level-set method [10], and the computational complexity is exponential in the dimension of the state. This leads to intractable computation for high-dimensional systems. On the other hand, PMP provides necessary conditions for optimality. The solution of PMP is either numerically computed by, e.g. shooting methods [11], or analytically derived. With shooting methods, computing the solutions to the PMP conditions is more tractable for higher-dimensional systems than the HJB approach. Furthermore, PMP yields sufficient conditions for convex optimal control problems [12], [13]. In the literature, PMP has been widely adopted to solve various constrained optimal control problems. It was first applied to aircraft control and fuel management [14], [15], and expanded to other areas such as hybrid electric vehicle energy management [16], train operation [17], fluid structures [18], and persistent monitoring in multi-agent systems [19].

In this paper, we focus on the PMP approach to analytically derive the optimal solution for the battery fast charging problem. This allows us to explicitly relate model parameters to the optimal input and state trajectories. We

---

Saehong Park, and Scott Moura are with the Energy, Controls and Applications Lab (eCAL) at the University of California, Berkeley, CA 94720, USA (E-mail: {sspark, smoura}@berkeley.edu)

Donggun Lee, and Claire Tomlin are with Hybrid Systems Lab at the University of California, Berkeley, CA 94720 (E-mail: {donggun\_lee, tomlin}@berkeley.edu)

Hyoung Jun Ahn is with LG Chem, BMS Advanced SW Project Team, Yuseong-gu, Daejeon, 305-738, South Korea (E-mail: ctz-nahj@lgchem.com)

examine a reduced-order electrochemical model, as this represents a physical interpretation of state constraints. Our contribution is to prove that battery fast charging, for a class of models, yields a solution that maximizes its allowable charging current until a safety constraint is active. When the safety constraint becomes active, then a feedback control law is applied to ensure safety. We derive analytical solutions from PMP and validate the proposed solutions by numerical simulation.

The paper is organized as follows. Section II briefly summarizes Pontryagin Minimum Principle in optimal control. Section III describes the electrochemical model. Section IV presents the optimal control problem formulation and analytical solution. In Section V, we summarize our work and provide perspectives on future work.

## II. PRELIMINARIES

This section introduces the Pontryagin Minimum Principle for optimal control problems [12], [20]–[22]. For a given dynamical system,

$$\dot{x} = f(x(t), u(t), t), \quad x(0) = x_0, \quad (1)$$

where  $x(t) \in \mathbb{R}^n$  and  $u(t) \in \mathbb{R}^m$ , and  $f : \mathbb{R}^n \times \mathbb{R}^m \times \mathbb{R} \rightarrow \mathbb{R}^n$  is assumed to be continuously differentiable in its arguments. The control input  $u(t)$  is *admissible* in a given time horizon if

$$u(t) \in \Omega(t) \subset \mathbb{R}^m, \quad t \in [0, t_f]. \quad (2)$$

The objective function is defined as

$$\mathcal{J} = h(x(t_f), t_f) + \int_0^{t_f} g(x(t), u(t), t) dt, \quad (3)$$

where  $g$  is the running cost,  $g : \mathbb{R}^n \times \mathbb{R}^m \times \mathbb{R} \rightarrow \mathbb{R}$  and  $h$  is terminal cost,  $h : \mathbb{R}^n \times \mathbb{R} \rightarrow \mathbb{R}$ . Both functions are continuously differentiable and  $t_f$  denotes the terminal time. The objective of the optimal control problem is to design  $u(t)$  to minimize the overall cost, mathematically,

$$\min_{u(\cdot)} \mathcal{J} : \dot{x} = f(x(t), u(t), t), x(0) = x_0, u(t) \in \Omega(t), \quad (4)$$

the optimal control problem is to find an admissible control  $u^*$ , which minimizes the objective function (3) subject to the state equation and the associated constraints. The control  $u^*$  is called an optimal control and  $x^*$  is called the *optimal trajectory*.

### A. Unconstrained Optimal Control

Without constraints on the inputs and states, we first derive the necessary conditions for (4). First, the Hamiltonian function,  $\mathcal{H} : \mathbb{R}^n \times \mathbb{R}^m \times \mathbb{R}^n \times \mathbb{R} \rightarrow \mathbb{R}$  is defined as:

$$\mathcal{H}(x, u, p, t) \triangleq g(x, u, t) + p^\top f(x, u, t), \quad (5)$$

where  $p \in \mathbb{R}^n$  is called the adjoint vector or the costate vector. The necessary conditions for  $u^*$  to be an optimal control are obtained by *Calculus of Variations*: for all  $u \in \Omega(t)$ ,  $t \in [0, T]$

$$\dot{x}^*(t) = \frac{\partial \mathcal{H}}{\partial p}(x^*(t), u^*(t), p(t), t), \quad (6)$$

$$\dot{p}(t) = -\frac{\partial \mathcal{H}}{\partial x}(x^*(t), u^*(t), p(t), t), \quad (7)$$

$$0 = \frac{\partial \mathcal{H}}{\partial u}(x^*(t), u^*(t), p(t), t), \quad (8)$$

with corresponding transversality or boundary conditions,

$$0 = \frac{\partial h}{\partial x}(x^*(t_f), t_f) - p(t_f), \quad (9)$$

$$0 = \mathcal{H}(x^*(t_f), u^*(t_f), p(t_f), t_f) + \frac{\partial h}{\partial t}(x^*(t_f), t_f). \quad (10)$$

With eqs. (7) and (9), we can determine the costate trajectory. Note that  $p(t_f) = 0$  when the terminal state is free or the terminal cost function  $h(\cdot)$  is zero. The conditions for optimality are also sufficient if  $\mathcal{H}$  is convex in  $(x, u)$  for each  $(p, t) \in \mathbb{R}^n \times [0, T]$  and  $h(x, t_f)$  is convex in  $x$  [12], [13].

### B. Constrained Optimal Control

Most control systems have constraints on inputs and states inherently. Based on the Hamiltonian function in (5), we add some of features of constraint functions to construct the constrained optimal control problem. First of all, the input  $u(t)$  is *admissible* if it is piecewise continuous and satisfies the mixed constraints, such as

$$l(x(t), u(t), t) \leq 0, \quad t \in [0, t_f], \quad (11)$$

where  $l : \mathbb{R}^n \times \mathbb{R}^m \times \mathbb{R} \rightarrow \mathbb{R}^q$  is continuously differentiable. In addition, we can consider pure state variable inequality constraints, namely,

$$c(x(t), t) \leq 0, \quad t \in [0, t_f], \quad (12)$$

where  $c : \mathbb{R}^n \times \mathbb{R} \rightarrow \mathbb{R}^{n_c}$ . For example, suppose states are required to be positive,  $x(t) \geq 0$ . In any interval where  $x(t) = 0$ , we must have  $\dot{x}(t) \geq 0$  so that  $x$  does not become negative. Lastly, the terminal state is constrained by inequality and equality constraints, namely

$$a(x(t_f), t_f) \leq 0, \quad (13)$$

$$b(x(t_f), t_f) = 0, \quad (14)$$

where  $a : \mathbb{R}^n \times \mathbb{R} \rightarrow \mathbb{R}^{n_a}$  and  $b : \mathbb{R}^n \times \mathbb{R} \rightarrow \mathbb{R}^{n_b}$  are continuously differentiable. The Lagrange function,  $\mathcal{L} : \mathbb{R}^n \times \mathbb{R}^m \times \mathbb{R}^n \times \mathbb{R}^q \times \mathbb{R}^{n_c} \times \mathbb{R} \rightarrow \mathbb{R}$  is defined as:

$$\mathcal{L}(x, u, p, \mu, \eta, t) \triangleq \mathcal{H}(x, u, p, t) + \mu^\top l(x, u, t) + \eta^\top c(x, t), \quad (15)$$

where  $\mu$  and  $\eta$  are Lagrange multipliers. When convenient, we omit the time argument for readability. Since the constraints are adjoined directly to form the Lagrangian, this method is called direct adjoining method. The Lagrange multipliers satisfy the complimentary slackness conditions, namely,

$$\mu(t) \geq 0, \quad \mu(t)^\top l(x, u, t) = 0, \quad (16)$$

$$\eta(t) \geq 0, \quad \eta(t)^\top c(x, t) = 0. \quad (17)$$

Pontryagin's Minimum Principle allows for a jump in  $p(t)$  at a point in time when the state  $x(t)$  enters its constraint boundary. The jump must satisfy the conditions

$$p(\tau^-) = p(\tau^+) + \zeta(\tau) \frac{\partial c}{\partial x}(x^*(\tau), \tau), \quad (18)$$

where  $\zeta(\tau) \geq 0$  and

$$\mathcal{H}(x^*(\tau), u^*(\tau^-), p(\tau^-), \tau) =$$

$$\mathcal{H}(x^*(\tau), u^*(\tau^+), p(\tau^+), \tau) - \zeta(\tau) \frac{\partial \mathcal{L}}{\partial t}(x^*(\tau), \tau), \quad (19)$$

at a time  $\tau$  at which one of the state variables has just reached its boundary value. An instant  $\tau$  is called *entry time* if there is an interior interval ending at  $t = \tau$  and a boundary interval starting at  $\tau$ . Similarly  $\tau$  is called an *exit time* if a boundary interval ends and an interior interval starts. If the trajectory just touches the boundary, then  $\tau$  is called *contact time*. Taken together, *entry*, *exit*, *contact* times are called *junction times*.

The necessary conditions for the optimality of  $u^*$  by using the *Calculus of Variations* [21] are obtained as follows:

$$\dot{x}^*(t) = \frac{\partial \mathcal{L}}{\partial p}(x^*(t), u^*(t), p(t), \mu(t), \eta(t), t), \quad (20)$$

$$\dot{p}(t) = -\frac{\partial \mathcal{L}}{\partial x}(x^*(t), u^*(t), p(t), \mu(t), \eta(t), t), \quad (21)$$

$$0 = \frac{\partial \mathcal{L}}{\partial u}(x^*(t), u^*(t), p(t)), \quad (22)$$

with corresponding transversality conditions,

$$0 = \frac{\partial h}{\partial x}(x^*(t_f), t_f) + \alpha \frac{\partial a}{\partial x}(x^*(t_f), t_f) + \beta \frac{\partial b}{\partial x}(x^*(t_f), t_f) + \gamma \frac{\partial c}{\partial x}(x^*(t_f), t_f) - p(t_f), \quad \alpha \geq 0 \quad (23)$$

$$0 = \gamma^\top c(x^*(t_f), t_f), \quad \gamma \geq 0, \quad (24)$$

the complimentary slackness conditions hold

$$\mu(t) \geq 0, \quad \mu(t)^\top l(x^*, u^*, t) = 0, \quad (25)$$

$$\eta(t) \geq 0, \quad \eta(t)^\top c(x^*(t), t) = 0, \quad (26)$$

$$\zeta(\tau) \geq 0, \quad \zeta(\tau) c(x^*(\tau), \tau) = 0, \quad (27)$$

and jump conditions (18)–(19) should hold at any entry/contact time  $\tau$ . Similar to the unconstrained case, if the Hamiltonian is convex with respect to  $(x, u)$ , then the conditions are also sufficient [12], [13].

### III. ELECTROCHEMICAL BATTERY MODEL

Electrochemical models achieve high accuracy and represent physical details of battery dynamics. We refer to the Doyle-Fuller-Newman (DFN) model as a “full-order model”. The DFN predicts the evolution of Lithium concentration for diffusion in the solid and liquid phases, as well as charge conservation in both electrodes [23]. On the other hand, “reduced-order models” are widely used for computational simplicity, analysis, and controller/observer design.

Over the past years, many researchers have studied model reduction techniques for the DFN model. The most commonly used reduced-order model is the single particle model (SPM), which idealizes each electrode as a single spherical porous particle, while neglecting electrolyte dynamics, as shown in Fig. 1. Specifically, the electrolyte concentration is approximated as constant in space and time, and this restriction causes errors which will be discussed later in this section. The intercalation process and mass transport is modeled by a linear diffusion PDE over spherical coordinates:

$$\frac{\partial c_s^\pm}{\partial t}(r, t) = \frac{1}{r^2} \frac{\partial}{\partial r} \left[ D_s^\pm r^2 \frac{\partial c_s^\pm}{\partial r}(r, t) \right], \quad (28)$$

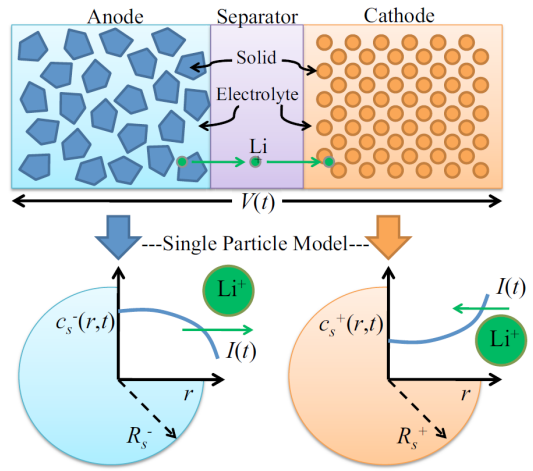


Figure 1: Schematic of single particle model.

with Neumann boundary conditions,

$$\frac{\partial c_s^\pm}{\partial r}(0, t) = 0, \quad \frac{\partial c_s^\pm}{\partial r}(R_s^\pm, t) = -\frac{1}{D_s^\pm} j_n^\pm, \quad (29)$$

where  $j_n$  is molar ion flux which is proportional to input current,  $I(t)$ ,

$$j_n^\pm = \mp \frac{I(t)}{F a^\pm A L^\pm}. \quad (30)$$

The Neumann boundary conditions at  $r = R_s^-$  and  $r = R_s^+$  represent that the molar flux of lithium entering / exiting the electrode, and is proportional to the input current  $I(t)$ . The description of each variable for SPM can be found in [24]. The terminal voltage output is governed by a combination of electric overpotential, electrode thermodynamics, and Butler-Volmer kinetics, yielding:

$$V(t) = \frac{RT}{\alpha^+ F} \sinh^{-1} \left( \frac{-I(t)}{2a^+ AL^+ i_0^+(c_{ss}^+(t))} \right) + \frac{RT}{\alpha^- F} \sinh^{-1} \left( \frac{I(t)}{2a^- AL^- i_0^-(c_{ss}^-(t))} \right) + U^+(c_{ss}^+(t)) - U^-(c_{ss}^-(t)) + R_f I(t), \quad (31)$$

where the exchange current density  $i_0^\pm$  and solid-electrolyte surface concentration  $c_{ss}^\pm$  are computed as:

$$i_0^\pm(c_{ss}^\pm) = k^\pm \sqrt{c_e^0 c_{ss}^\pm(t) (c_{s,\max}^\pm - c_{ss}^\pm(t))}, \quad (32)$$

$$c_{ss}^\pm(t) = c_s^\pm(R_s^\pm, t). \quad (33)$$

In this model, SOC is defined as the normalized volume sum of lithium concentration in the anode:

$$SOC_n = \frac{3}{c_{s,\max}^-(R_s^-)^3} \int_0^{R_s^-} r^2 c_s^-(r, t) dr. \quad (34)$$

There are numbers of techniques to discretize PDE (28) in the literature [25]–[29]. Among them, we apply Padé approximation [29] to the solid-phase diffusion PDE (28). We briefly explain Padé approximation next, since the optimal control solution is based on this discretized model. By taking the Laplace transform from input  $j_n$  to  $c_s^\pm(R_s^\pm, s)$ , the PDE (28)–(29) is written as a transcendental transfer function:

$$G(s) = \frac{c_s^\pm(R_s^\pm, s)}{j_n(s)}$$

$$= \frac{R_s^\pm}{D_s^\pm} \frac{\sinh\left(\sqrt{\frac{s}{D_s^\pm}} R_s^\pm\right)}{R_s^\pm \sqrt{\frac{s}{D_s^\pm}} \cosh\left(\sqrt{\frac{s}{D_s^\pm}} R_s^\pm\right) - \sinh\left(\sqrt{\frac{s}{D_s^\pm}} R_s^\pm\right)}. \quad (35)$$

The third-order Padé approximation of (35) is:

$$G(s) \approx \frac{\frac{3}{R_s^\pm} + \frac{4R_s^\pm}{11D_s^\pm} s + \frac{R_s^{\pm 3}}{165D_s^{\pm 2}} s^2}{s\left(1 + \frac{3R^2}{55D_s} s + \frac{R^4}{3465D_s^2} s^2\right)}. \quad (36)$$

Then, the controllable canonical state-space form is:

$$\begin{bmatrix} \dot{c}_{s1}^\pm \\ \dot{c}_{s2}^\pm \\ \dot{c}_{s3}^\pm \end{bmatrix} = \begin{bmatrix} 0 & 1 & 0 \\ 0 & 0 & 1 \\ 0 & -\frac{3465D_s^{\pm 2}}{R_s^{\pm 4}} & -\frac{189D_s^\pm}{R_s^{\pm 2}} \end{bmatrix} \begin{bmatrix} c_{s1}^\pm \\ c_{s2}^\pm \\ c_{s3}^\pm \end{bmatrix} + \begin{bmatrix} 0 \\ 0 \\ \frac{3465D_s^{\pm 2}}{R_s^{\pm 4}} \end{bmatrix} j_n^\pm \quad (37)$$

$$c_s^\pm(R_s^\pm, s) = \left[ \frac{3}{R_s^\pm} \quad \frac{4R_s^\pm}{11D_s^\pm} \quad \frac{R_s^{\pm 3}}{165D_s^{\pm 2}} \right]. \quad (38)$$

Lastly, we can derive the state-space realization where the bulk concentration,  $\bar{c}_s^- = SOC_n \cdot c_{s,\max}^-$  is expressed as a state in a Jordan-form. We perform *linear transformation* such that the system matrix has diagonal form,

$$\dot{x} = Ax + Bu,$$

where

$$A = \begin{bmatrix} a_1 & 0 & 0 \\ 0 & a_2 & 0 \\ 0 & 0 & 0 \end{bmatrix}, \quad B = \begin{bmatrix} b_1 \\ b_2 \\ b_3 \end{bmatrix}, \quad (39)$$

and we define surface concentration,  $c_{ss}^- = C^\top x$ , as an output function of the states,  $x = [x_1, x_2, x_3]^\top$ , and bulk concentration for the anode is a state,  $\bar{c}_s^- = x_3$ .

$$\bar{c}_{ss}^- = \left[ \frac{3}{R_s^-} \quad \frac{4R_s^-}{11D_s^-} \quad \frac{(R_s^-)^3}{165(D_s^-)^2} \right] x = C^\top x. \quad (40)$$

Table I shows the values of the A, B, C matrices for several common Li-ion chemistries. Note that the sign of the elements are consistent, which is important for generalizing the optimal control solutions across chemistries.

	LCO <sup>†</sup>	NCA <sup>‡</sup>	NMC <sup>‡‡</sup>
$a_1$	-7.3E-02	-1.2E-02	-3.4E-01
$a_2$	-8.9E-03	-1.47E-03	-4.2E-02
$B$	$\begin{bmatrix} 6.5E-07 \\ -8.0E-08 \\ -1.7E-01 \end{bmatrix}$	$\begin{bmatrix} 2.4E-05 \\ -3.0E-06 \\ -3.2 \end{bmatrix}$	$\begin{bmatrix} 2.2E-07 \\ -2.7E-08 \\ -1.2E-01 \end{bmatrix}$
$C$	$\begin{bmatrix} -1.3E+06 \\ 1.5E+06 \\ 1 \end{bmatrix}$	$\begin{bmatrix} -6.8E+05 \\ 7.7E+05 \\ 1 \end{bmatrix}$	$\begin{bmatrix} -2.9E+06 \\ 3.3E+06 \\ 1 \end{bmatrix}$

<sup>†</sup>Lithium Cobalt Oxide [30], <sup>‡</sup>Nickel Cobalt Aluminum Oxide [23]

<sup>‡‡</sup>Nickel Manganese Cobalt Oxide

Table I: A, B, and C matrices for three common battery chemistries.

#### IV. FAST CHARGING OPTIMAL SOLUTION

In this section, we derive the optimal solution for the fast charging problem. First, we start with the Single Particle Model (SPM) optimal control problem formulated as follows:

$$\begin{aligned} & \max_{u(t)} \int_{t_0}^{t_f} x_3(t) dt & (41) \\ \text{subject to} & \quad \dot{x}_1 = a_1 x_1 + b_1 u, & x_1(0) = x_{10}, \\ & \quad \dot{x}_2 = a_2 x_2 + b_2 u, & x_2(0) = x_{20}, \\ & \quad \dot{x}_3 = b_3 u, & x_3(0) = x_{30}, \\ & \quad -u_b \leq u \leq u_b, \\ & \quad C^\top x \leq C_b, \end{aligned}$$

where  $-u_b$  represents the maximum charging rate, and the state constraint places an upper bound on the surface concentration in (40), denoted by  $C_b$ . The surface concentration cannot exceed its maximum concentration level,  $c_{s,\max}^-$ , which is determined by the electrode's electrochemical properties. The objective is to maximize the bulk concentration of the anode, in a fixed time horizon, in the presence of input and state constraints. Note that  $h(x(t_f), t_f) = a(x(t_f), t_f) = b(x(t_f), t_f) = 0$  in (3), (13), (14). Our objective is to characterize the battery fast charging problem by using Pontryagin Minimum Principle. The necessary optimal conditions discussed in Section II are computed as follows. The Lagrangian is:

$$\begin{aligned} \mathcal{L} &= x_3 + p^\top (Ax + Bu) \\ &+ \mu_1(u + u_b) + \mu_2(u_b - u) + \eta(C_b - C^\top x). \end{aligned} \quad (42)$$

where  $p = [p_1, p_2, p_3]^\top$  is the co-state vector, and  $\mu_1, \mu_2, \eta$  are Lagrange multipliers associated with input and state constraints. Note that  $\mu_1, \mu_2$  do not affect the sign of  $\mathcal{L}$  due to the complimentary slackness. To find the optimal control solution, we focus on the part of  $\mathcal{L}$  that depends on  $u$

$$\tilde{\mathcal{L}} = (b_1 p_1 + b_2 p_2 + b_3 p_3) u + (\mu_1 - \mu_2) u, \quad (43)$$

The costate dynamics (21) and input optimality (22) are computed as

$$\dot{p}_1(t) = -a_1 p_1 + \eta c_1, \quad (44)$$

$$\dot{p}_2(t) = -a_2 p_2 + \eta c_2, \quad (45)$$

$$\dot{p}_3(t) = -1 + \eta c_3, \quad (46)$$

$$0 = p_1 b_1 + p_2 b_2 + p_3 b_3 + \mu_1 - \mu_2. \quad (47)$$

Next, we state the two main results of this paper. They describe the optimal solution with inactive constraints and active constraints, which respectively give *Bang* and *Bang-Ride* solutions. First of all, the state trajectory for maximum charging current can be derived analytically:

$$x_1(t) = e^{a_1 t} x_1(0) + \frac{b_1 u_b}{a_1} (1 - e^{a_1 t}), \quad (48)$$

$$x_2(t) = e^{a_2 t} x_2(0) + \frac{b_2 u_b}{a_2} (1 - e^{a_2 t}), \quad (49)$$

$$x_3(t) = -b_3 u_b t + x_3(0). \quad (50)$$

The range of  $C_b$  that yields an unconstrained optimal control solution to (41) is given by:

$$c_1 x_1(t_f) + c_2 x_2(t_f) + c_3 x_3(t_f) \triangleq \bar{C} < C_b. \quad (51)$$

**Theorem 1.** If  $C_b > \bar{C}$ , then the optimal solution to (41) is to maximize the current input,  $-u_b$ , so-called Bang control, and the state constraint is not active during the control horizon.

*Proof:* Inactive state constraint implies that  $\gamma = 0$  in transversality conditions (23), (24) and the Lagrange multiplier,  $\eta(\cdot) \equiv 0$ . Then, we can find the final conditions of co-states  $p(t)$  at terminal time by solving co-state dynamical equations in (44) – (46), such as:

$$\begin{aligned} p_1(t_f) = p_2(t_f) = p_3(t_f) = 0, \\ \iff p_1(0) = p_2(0) = 0, p_3(0) = t_f. \end{aligned}$$

Therefore, the co-state trajectories are:

$$p_1(t) = p_2(t) = 0, \quad p_3(t) = -t + t_f.$$

We find that (43) is maximized when  $u = -u_b$ , which implies that the optimal current is the maximum charging rate. ■

**Theorem 2.** If  $C_b < \bar{C}$ , then the optimal solution to (41) is to maximize the current input,  $-u_b$ , until the inequality constraint becomes active. Then it rides the constraint bound – Bang-Ride control. Furthermore, the switching time<sup>1</sup>,  $\sigma$ , does not exist for  $C_b < \bar{C}$  but the Junction time,  $\tau$ , exists.

*Proof:* To prove this theorem, we consider two cases: 1) when the state constraint becomes active at the terminal time, 2) when the state constraint becomes active prior to the terminal time.

**Case 1:** Consider the case when the state constraint becomes active at the terminal time, which implies that  $\gamma \neq 0$ . Then the transversality condition (23) yields

$$\begin{aligned} p_1(t_f) &= -c_1\gamma, \\ p_2(t_f) &= -c_2\gamma, \\ p_3(t_f) &= -c_3\gamma, \end{aligned}$$

with the final conditions above, the co-state trajectories become a function of  $\gamma$ , such as,

$$p_1(t) = \frac{-c_1\gamma}{e^{-a_1 t_f}} e^{-a_1 t}, \quad (52)$$

$$p_2(t) = \frac{-c_2\gamma}{e^{-a_2 t_f}} e^{-a_2 t}, \quad (53)$$

$$p_3(t) = -t - c_3\gamma + t_f. \quad (54)$$

Plugging this into  $b_1 p_1 + b_2 p_2 + b_3 p_3$  in (43), then the switching time occurs when the sign of (43) changes. That is, the optimal current input switches from  $-u_b$  to  $+u_b$ . The existence of a switching time  $\sigma$  is equivalent to the existence of a root of  $b_1 p_1 + b_2 p_2 + b_3 p_3 = 0$  w.r.t.  $t$ , namely:

$$\gamma \left( \frac{-b_1 c_1}{e^{-a_1 t_f}} e^{-a_1 t} + \frac{-b_2 c_2}{e^{-a_2 t_f}} e^{-a_2 t} - b_3 c_3 \right) = b_3(t - t_f). \quad (55)$$

The range of  $\gamma$  that yields a solution  $t = \sigma(\gamma)$  to (55) is

$$0 \leq \gamma \leq \frac{-b_3 t_f}{\frac{-b_1 c_1}{e^{-a_1 t_f}} + \frac{-b_2 c_2}{e^{-a_2 t_f}} - b_3 c_3} \approx t_f. \quad (56)$$

Then the Bang-Bang control law is obtained as follows:

$$u^*(t) = \begin{cases} -u_b, & t \leq \sigma(\gamma), \\ +u_b, & t > \sigma(\gamma), \end{cases} \quad (57)$$

and the state trajectory is computed as:

$$x_1(t) = \begin{cases} e^{a_1 t} x_1(0) + \frac{b_1 u_b}{a_1} (1 - e^{a_1 t}), & t \leq \sigma(\gamma), \\ e^{a_1 (t - \sigma(\gamma))} x_1(\sigma(\gamma)) - \frac{b_1 u_b}{a_1} (1 - e^{a_1 (t - \sigma(\gamma))}), & t > \sigma(\gamma), \end{cases} \quad (58)$$

$$x_2(t) = \begin{cases} e^{a_2 t} x_2(0) + \frac{b_2 u_b}{a_2} (1 - e^{a_2 t}), & t \leq \sigma(\gamma), \\ e^{a_2 (t - \sigma(\gamma))} x_2(\sigma(\gamma)) - \frac{b_2 u_b}{a_2} (1 - e^{a_2 (t - \sigma(\gamma))}), & t > \sigma(\gamma), \end{cases} \quad (59)$$

$$x_3(t) = \begin{cases} -b_3 u_b t + x_3(0), & t \leq \sigma(\gamma), \\ b_3 u_b (t - \sigma(\gamma)) + x_3(\sigma(\gamma)), & t > \sigma(\gamma). \end{cases} \quad (60)$$

We claim that  $\sigma(\gamma)$  does not exist as the state constraint is violated before  $t$  reaches  $\sigma(\gamma)$ . That is  $C^\top x(\sigma) > C^\top x(t_f), \forall \sigma(\gamma)$ . Note that  $\sigma(\gamma)$  is determined by  $\gamma$  in (56), then the constraint bound,  $C_b$  is obtained as  $C^\top x(t_f)$ , where  $x(t_f)$  follows from (58) – (60). We can check that the following statement holds for given ranges of electrochemical values in Table I :

$$\begin{aligned} c_1 [(e^{a_1 (t_f - \sigma)} - 1) x_1(\sigma) - \frac{b_1 u_b}{a_1} (1 - e^{a_1 (t_f - \sigma)})] \\ + c_2 [(e^{a_2 (t_f - \sigma)} - 1) x_2(\sigma) - \frac{b_2 u_b}{a_2} (1 - e^{a_2 (t_f - \sigma)})] \\ + c_3 [b_3 u_b (t_f - \sigma)] < 0. \end{aligned} \quad (61)$$

We conclude that the switching time does not exist when the state constraint becomes active at the terminal time. The switching time occurs only if  $C_b = \bar{C}$ , and is equivalent to terminal time,  $t_f$ . Note that we speculated that the state constraint becomes active when the constraint  $C_b$  is less than  $\bar{C}$ , which is the scenario discussed in Case 2 next.

**Case 2:** Consider the case when the state constraint becomes active prior to the terminal time. Then transversality condition (23) and junction condition (18) state that

$$p(t_f) = -\gamma C, \quad (62)$$

$$p(\tau^-) = p(\tau^+) + \zeta(-C), \quad (63)$$

where  $t = \tau$  is the time when the state hits the state constraint bound,

$$C^\top x(\tau) = C_b. \quad (64)$$

Then the input  $u$  can be found such that state does not violate the constraint further, i.e.,  $C^\top \dot{x}(t) = 0 \forall t \in [\tau^+, t_f]$ . We can find such an input by taking time derivative of the state constraint function,

$$\begin{aligned} 0 &= C^\top \dot{x}, \\ &= C^\top (Ax + Bu), \end{aligned} \quad (65)$$

then the input  $u(t)$  becomes a state feedback control law:

$$u(t) = -\frac{C^\top A}{C^\top B} x \triangleq -Kx, \quad (66)$$

where  $K \in \mathbb{R}^{1 \times 3}$ . Note that the input  $u$  is potentially discontinuous at  $t = \tau$ . Plugging the feedback control

<sup>1</sup>switching refers to shift other extreme value, e.g.,  $-u_b \rightarrow u_b$ .

law into the dynamical system results in the following autonomous system:

$$\dot{x}(t) = (A - BK)x(t), \quad t \in [\tau^+, t_f]. \quad (67)$$

We claim that the feedback control law (66) is bounded for the input constraint, namely

$$-u_b < -Kx(t) < u_b. \quad (68)$$

The system is autonomous for  $t \in [\tau^+, t_f]$  such that  $x(t)$  can be analytically derived,

$$-u_b < -Ke^{(A-BK)t}x_0 < u_b, \quad t \in [\tau^+, t_f]. \quad (69)$$

Notice that  $|-Ke^{(A-BK)t}x_0| \leq |-Kx_0|, \forall t \in [\tau^+, t_f]$  as  $\text{eig}(A - BK) \leq 0$  for given electrochemical model. A bounded feedback control law ensures the Lagrange multipliers associated with input constraints are zero, i.e.,  $\mu_1 = 0, \mu_2 = 0$  due to complimentary slackness. Then (47) becomes

$$p^\top(t)B = 0, \quad t \in [\tau, t_f]. \quad (70)$$

We aim to find  $\gamma$  at terminal time  $t = t_f$ ,

$$0 = p^\top(t_f)B = -\gamma C^\top B, \quad (71)$$

since  $C^\top B \neq 0, \gamma = 0$ . For the constrained optimal control case, we divide the time horizon into two cases i) state constraint is not active, i.e.,  $t \in [0, \tau]$  ii) state constraint becomes active, i.e.,  $t \in [\tau^+, t_f]$ .

The next step is to compute the co-state trajectory for the following input,

$$u^*(t) = \begin{cases} -u_b, & t \in [0, \tau], \\ -Kx, & t \in [\tau^+, t_f], \end{cases} \quad (72)$$

then the costate trajectory is obtained as follows:

$$p(t) = \begin{cases} e^{-At}p(0) + [0, 0, -t]^\top, & t \in [0, \tau], \\ [e^{\bar{A}(t_f-t)} - \mathbb{I}] \theta, & t \in [\tau^+, t_f], \end{cases} \quad (73)$$

where

$$\bar{A} = \left( I - \frac{CB^\top}{B^\top C} \right) A, \quad \theta = \begin{bmatrix} -\frac{c_1}{a_1 c_3} \\ -\frac{a_1 c_3}{a_2 c_3} \\ 0 \end{bmatrix}. \quad (74)$$

The derivation of the co-state trajectory for  $t \in [\tau, t_f]$  is not trivial, so it is relegated to the Appendix. Given an allowable maximum current, i.e.  $u_b \geq |-Kx_0|$ , we find the junction time  $\tau$  when the state constraint becomes active, i.e.

$$c_1 x_1(\tau) + c_2 x_2(\tau) + c_3 x_3(\tau) = C_b. \quad (75)$$

Then we construct algebraic equations for unknowns  $\zeta, p(0)$  from 1) jump condition form of co-states in (18), 2) jump condition for Hamiltonian in (19), such as,

$$e^{-A\tau}p(0) + \begin{bmatrix} 0 \\ 0 \\ -\tau \end{bmatrix} = [e^{\bar{A}(t_f-\tau)} - \mathbb{I}] \theta + \zeta(\tau)C, \quad (76)$$

$$\left[ e^{-A\tau}p(0) + \begin{bmatrix} 0 \\ 0 \\ -\tau \end{bmatrix} \right]^\top (Ax(\tau) + Bu(\tau^-))$$

$$= \left[ (e^{\bar{A}(t_f-\tau)} - \mathbb{I}) \theta \right]^\top (Ax(\tau) + Bu(\tau^+)), \quad (77)$$

where

$$u(\tau^-) = -u_b, \quad u(\tau^+) = -\frac{C^\top Ax(\tau)}{C^\top B}.$$

Then, the analytical solution of  $\zeta$  is obtained as follows:

$$\zeta(\tau) = \frac{\left[ (e^{\bar{A}(t_f-\tau)} - \mathbb{I}) \theta \right]^\top B \left( -\frac{C^\top Ax(\tau)}{C^\top B} + u_b \right)}{C^\top (Ax(\tau) - Bu_b)}. \quad (78)$$

With  $\zeta(t)$  computed above, the boundary condition for costate,  $p_0$  can be obtained as:

$$p(0) = e^{A\tau} \left( [e^{\bar{A}(t_f-\tau)} - \mathbb{I}] \theta + \zeta(\tau)C + \begin{bmatrix} 0 \\ 0 \\ \tau \end{bmatrix} \right). \quad (79)$$

Lastly, we check whether a switching time exists for  $t \in [0, \sigma]$ . First,  $\tau$  is chosen between  $\tau \in [0, t_f]$ , then  $C_b$  is obtained by  $C_b = C^\top x(\tau)$ . By solving the algebraic equations (76) – (77), we find  $p_0$ , and then check that  $b_1 p_1(t) + b_2 p_2(t) + b_3 p_3(t) \leq 0$  for  $\tau, t \in [0, t_f]$  for given electrochemical parameters described in Table I. ■

Therefore, when the state constraint becomes active prior to the terminal time, the optimal control input is to apply state feedback control law (66), which results in riding the constraints boundary.

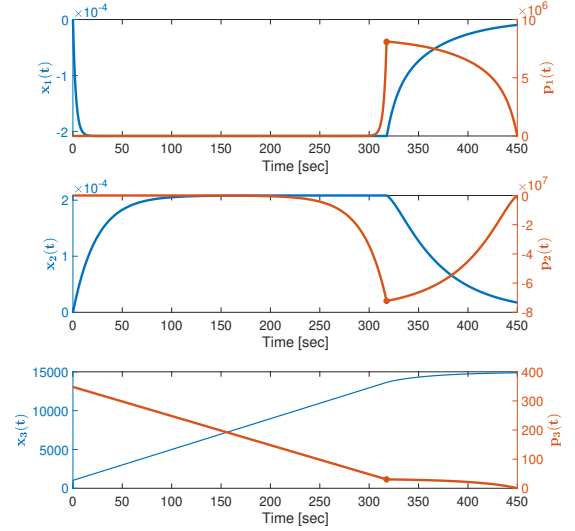
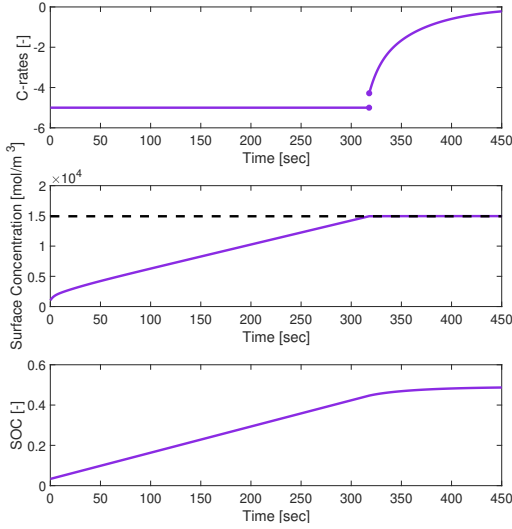
**Remark 1.** The optimal solution for  $u(t)$  in (41) is the global optimal solution as the necessary conditions become necessary and sufficient conditions because (41) is convex.

The analytical solution of the optimal input, state trajectory, co-state trajectory, and associated Lagrange multipliers for the constrained optimal control problem are summarized in Table II.

Interval	$t \in [0, \tau]$	$t \in [\tau, t_f]$
$u(t)$	$-u_b$	$-Kx$
$x(t)$	$e^{At}x_0 - \int_0^t e^{A(t-s)}Bu_b ds$	$e^{(A-BK)(t-\tau)}x(\tau)$
$p(t)$	$e^{-At}p(0) + [0 \quad 0 \quad -t]^\top$	$[e^{\bar{A}(t_f-t)} - \mathbb{I}] \theta$
$\mu_1(t)$	$-p^\top(t)B$	0
$\mu_2(t)$	0	0
$\eta(t)$	0	$\frac{B^\top A}{B^\top C} p(t) + \eta(t_f)$

Table II: The analytical solution of constrained optimal control problem (41) for  $C_b \leq \bar{C}$ . Unknown variables,  $\zeta, p(0)$ , and  $\eta(t_f)$  are derived in (78), (79), (84).

Numerical simulation results for the optimal fast charging problem (41) are presented in Fig. 2 to validate the proposed analytical solution. The terminal time,  $t_f$ , is chosen as 450 seconds, allowable maximum current,  $u_b$ , is 5 C-rate, and constraint bound,  $C_b$  is chosen as 50% of maximum concentration level (for illustration). The constrained optimal control solution satisfies  $C_b < \bar{C}$  from (51), and thus the junction time occurs at  $t = \tau = 317$ . Figure 2a displays the optimal input, state constraint activation, and the normalized objective function, which is SOC from (34). Figure 2b exhibits the corresponding trajectories for the states and co-states. Although difficult to see in the plots, the co-states are discontinuous at the junction time, and the trajectories satisfy the optimality conditions.



(a) Input, state constraint, and normalized objective function.

(b) States and co-states trajectories.

Figure 2: Numerical constrained optimal control results using analytical solutions in Table II.

## V. CONCLUSION

In this work, we analyze optimal fast charging control of Li-ion batteries. Pontryagin's Minimum Principle is used to derive the optimality conditions. We prove that the optimal fast-charging control is a *Bang-Ride* control, which applies maximum allowable charging current until the state constraint becomes active, and then rides the constraint bound to ensure safety. PMP analysis provides theoretical evidence why optimal fast-charging protocols are Bang-Ride control in the literature, at least for single particle models. Furthermore, our theoretical proofs can explain why specific constant current-constant voltage (CCCV) protocols are candidates for optimal for experimental design in fast charging problem [31], different experimental current pulse profiles [32], and fast charging method design [33]. Due to this analysis, the search space for optimal control solutions can be reduced to *Bang-Ride* trajectories without loss of optimality. On-going work involves extending PMP analysis for more sophisticated electrochemical models that are nonlinear with multiple constraints.

## VI. ACKNOWLEDGEMENTS

This research is funded by LG Chem Battery Innovative Contest. The authors thank the LG Chem researchers for their support and discussion in the work.

## VII. APPENDIX

In this appendix, the analytical solution of costate dynamics for  $t \in [\tau, t_f]$  is derived. The ODEs for the costates are  $\dot{p}_1 = -p_1 a_1 + \eta c_1$ ,  $\dot{p}_2 = -p_1 a_2 + \eta c_2$ ,  $\dot{p}_3 = -1 + \eta c_3$ , (80)

where  $\eta \geq 0$ . It is obvious that  $\eta(t) = 0$  if  $t \leq \tau^-$  due to complimentary slackness. We also have  $\gamma = 0$  as described in (71) Then,

$$p(t_f) = 0 \in \mathbb{R}^3. \quad (81)$$

From (70), (80) can be written as:

$$0 = B^T \dot{p}(t) = B^T \left( -Ap(t) + \begin{bmatrix} 0 \\ 0 \\ -1 \end{bmatrix} + \eta C \right), \quad (82)$$

thus we can compute  $\eta(t)$  such as:

$$\eta(t) = \frac{B^T A}{B^T C} p(t) + \eta(t_f), \quad (83)$$

where

$$\eta(t_f) := \frac{B^T [0 \ 0 \ 1]^T}{B^T C}. \quad (84)$$

Substituting (83) to (80), we obtain

$$\dot{p} = -Ap + \begin{bmatrix} 0 \\ 0 \\ -1 \end{bmatrix} + \left( \frac{B^T A}{B^T C} p(t) + \eta(t_f) \right) C. \quad (85)$$

We can design a constant vector

$$\theta = \left[ -\frac{c_1}{a_1 c_3} \quad -\frac{c_2}{a_2 c_3} \quad 0 \right]^T, \quad (86)$$

such that the following costate equation is derived.

$$p(t) = [e^{\bar{A}(t_f-t)} - I] \theta. \quad (87)$$

where  $\bar{A}$  is defined in (74).

## REFERENCES

- [1] R. Klein, N. A. Chaturvedi, J. Christensen, J. Ahmed, R. Findeisen, and A. Kojic, "Optimal charging strategies in lithium-ion battery", in *American Control Conference (ACC), 2011*, IEEE, 2011, pp. 382–387.
- [2] M. Torchio, N. A. Wolff, D. M. Raimondo, L. Magni, U. Kreuer, R. B. Gopaluni, J. A. Paulson, and R. D. Braatz, "Real-time model predictive control for the optimal charging of a lithium-ion battery", in *2015 American Control Conference (ACC)*, IEEE, 2015, pp. 4536–4541.
- [3] H. E. Perez, X. Hu, S. Dey, and S. J. Moura, "Optimal charging of li-ion batteries with coupled electro-thermal-aging dynamics", *IEEE Transactions on Vehicular Technology*, vol. 66, no. 9, pp. 7761–7770, 2017.
- [4] A. Pozzi, M. Torchio, and D. M. Raimondo, "Film growth minimization in a li-ion cell: A pseudo two dimensional model-based optimal charging approach", in *2018 European Control Conference (ECC)*, IEEE, 2018, pp. 1753–1758.

- [5] B. Suthar, P. W. Northrop, R. D. Braatz, and V. R. Subramanian, "Optimal charging profiles with minimal intercalation-induced stresses for lithium-ion batteries using reformulated pseudo 2-dimensional models", *Journal of The Electrochemical Society*, vol. 161, no. 11, F3144–F3155, 2014.
- [6] J. Liu, G. Li, and H. K. Fathy, "An extended differential flatness approach for the health-conscious nonlinear model predictive control of lithium-ion batteries", *IEEE Transactions on Control Systems Technology*, vol. 25, no. 5, pp. 1882–1889, 2017.
- [7] C. Zou, X. Hu, Z. Wei, T. Wik, and B. Egardt, "Electrochemical estimation and control for lithium-ion battery health-aware fast charging", *IEEE Transactions on Industrial Electronics*, vol. 65, no. 8, pp. 6635–6645, 2018.
- [8] R. Romagnoli, L. D. Couto, A. Goldar, M. Kinnaert, and E. Garone, "A feedback charge strategy for li-ion battery cells based on reference governor", *Journal of process control*, vol. 83, pp. 164–176, 2019.
- [9] A. Altarovici, O. Bokanowski, and H. Zidani, "A general hamilton-jacobi framework for non-linear state-constrained control problems", *ESAIM: Control, Optimisation and Calculus of Variations*, vol. 19, no. 2, pp. 337–357, 2013.
- [10] S. Osher and R. Fedkiw, *Level Set Methods and Dynamic Implicit Surfaces*. Springer-Verlag, 2003, vol. 153. DOI: 10.1007/b98879.
- [11] G. Lastman, "A shooting method for solving two-point boundary-value problems arising from non-singular bang-bang optimal control problems", *International journal of control*, vol. 27, no. 4, pp. 513–524, 1978.
- [12] R. F. Hartl, S. P. Sethi, and R. G. Vickson, "A survey of the maximum principles for optimal control problems with state constraints", *SIAM review*, vol. 37, no. 2, pp. 181–218, 1995.
- [13] O. L. Mangasarian, "Sufficient conditions for the optimal control of nonlinear systems", *SIAM Journal on control*, vol. 4, no. 1, pp. 139–152, 1966.
- [14] A. E. Bryson Jr, W. F. Denham, and S. E. Dreyfus, "Optimal programming problems with inequality constraints", *AIAA journal*, vol. 1, no. 11, pp. 2544–2550, 1963.
- [15] J. W. Burrows, "Fuel-optimal aircraft trajectories with fixed arrival times", *Journal of Guidance, Control, and Dynamics*, vol. 6, no. 1, pp. 14–19, 1983.
- [16] N. Kim, S. Cha, and H. Peng, "Optimal control of hybrid electric vehicles based on pontryagin's minimum principle", *IEEE Transactions on control systems technology*, vol. 19, no. 5, pp. 1279–1287, 2010.
- [17] E. Khmelnitsky, "On an optimal control problem of train operation", *IEEE transactions on automatic control*, vol. 45, no. 7, pp. 1257–1266, 2000.
- [18] P. Paoletti and L. Mahadevan, "Planar controlled gliding, tumbling and descent", *Journal of fluid mechanics*, vol. 689, pp. 489–516, 2011.
- [19] Y.-W. Wang, Y.-W. Wei, X.-K. Liu, N. Zhou, and C. G. Cassandras, "Optimal persistent monitoring using second-order agents with physical constraints", *IEEE Transactions on Automatic Control*, vol. 64, no. 8, pp. 3239–3252, 2018.
- [20] L. S. Pontryagin, *Mathematical theory of optimal processes*. Routledge, 2018.
- [21] D. E. Kirk, *Optimal control theory: an introduction*. Courier Corporation, 2004.
- [22] A. E. Bryson, *Applied optimal control: optimization, estimation and control*. Routledge, 2018.
- [23] S. Park, D. Kato, Z. Gima, R. Klein, and S. Moura, "Optimal experimental design for parameterization of an electrochemical lithium-ion battery model", *Journal of The Electrochemical Society*, vol. 165, no. 7, A1309–A1323, 2018.
- [24] S. Park, D. Zhang, and S. Moura, "Hybrid electrochemical modeling with recurrent neural networks for li-ion batteries", in *American Control Conference (ACC), 2017*, IEEE, 2017, pp. 3777–3782.
- [25] L. Cai and R. E. White, "Reduction of model order based on proper orthogonal decomposition for lithium-ion battery simulations", *Journal of the Electrochemical Society*, vol. 156, no. 3, A154–A161, 2009.
- [26] G. Fan, K. Pan, and M. Canova, "A comparison of model order reduction techniques for electrochemical characterization of lithium-ion batteries", in *2015 54th IEEE Conference on Decision and Control (CDC)*, IEEE, 2015, pp. 3922–3931.
- [27] S. J. Moura, "Estimation and control of battery electrochemistry models: A tutorial", in *2015 54th IEEE Conference on Decision and Control (CDC)*, IEEE, 2015, pp. 3906–3912.
- [28] C. Mayhew, W. He, C. Kroener, R. Klein, N. Chaturvedi, and A. Kojić, "Investigation of projection-based model-reduction techniques for solid-phase diffusion in li-ion batteries", in *2014 American Control Conference*, IEEE, 2014, pp. 123–128.
- [29] J. C. Forman, S. Bashash, J. L. Stein, and H. K. Fathy, "Reduction of an electrochemistry-based li-ion battery model via quasi-linearization and pade approximation", *Journal of the Electrochemical Society*, vol. 158, no. 2, A93–A101, 2011.
- [30] J. Newman, "Fortran programs for the simulation of electrochemical systems: Dualfoil5. 2. f (2014)", URL <http://www.cchem.berkeley.edu/jsngrp>,
- [31] P. M. Attia, A. Grover, N. Jin, K. A. Severson, T. M. Markov, Y.-H. Liao, M. H. Chen, B. Cheong, N. Perkins, Z. Yang, *et al.*, "Closed-loop optimization of fast-charging protocols for batteries with machine learning", *Nature*, vol. 578, no. 7795, pp. 397–402, 2020.
- [32] F. Savoye, P. Venet, M. Millet, and J. Groot, "Impact of periodic current pulses on li-ion battery performance", *IEEE Transactions on Industrial Electronics*, vol. 59, no. 9, pp. 3481–3488, 2011.
- [33] Y. Yin, Y. Hu, S.-Y. Choe, H. Cho, and W. T. Joe, "New fast charging method of lithium-ion batteries based on a reduced order electrochemical model considering side reaction", *Journal of Power Sources*, vol. 423, pp. 367–379, 2019.